Metamagnetism in single-crystal Pr_2NiO_4

M. T. Fernández-Díaz,* J. L. Martínez,* and J. Rodríguez-Carvajal†
Institut Laue-Langevin, Boîte Postale 156, F-38042 Grenoble-CEDEX-9, France

J. Beille
Laboratoire L. Néel, Boîte Postale 166, F-38042 Grenoble-CEDEX, France

B. Martínez and X. Obradors
Institut de Ciència de Materials de Barcelona, Consejo Superior de Investigaciones Cientificas Campus U. Autónoma, E-08193 Bellaterra, Barcelona, Spain

P. Odier
Centre de Recherches sur la Physique des Hautes Températures, F-45071 Orléans-CEDEX 2, France
(Received 20 April 1992; revised manuscript received 12 October 1992)

A study of the magnetic behavior of Pr_2NiO_4 single crystals is presented. Single-crystal neutron diffraction, magnetic susceptibility, and isothermal magnetization at various temperatures and magnetic fields applied along the different crystallographic axes are used to obtain an overall picture of the magnetic behavior. The metamagnetic transition is studied for temperatures below the structural phase transition ($T_{C1} \approx 117$ K). Between 1.5 K and T_{C1} the dependence of the spin arrangement with magnetic field is presented, and an H-T phase diagram is proposed. Above T_{C1} and up to the Néel temperature ($T_N \approx 325$ K) the system behaves as an antiferromagnet with the magnetic moments along the x direction.

I. INTRODUCTION

The system $R_2MO_{4+\delta}$ (R =La, Pr, Nd, Sm or Gd; M =Cu, Ni or Co) is an excellent system for studying the relationship between structural, magnetic, and transport properties. Depending on the relation between the transition metal (Cu, Ni, or Co) and the oxygen content, the system varies from insulator to superconductor.

The structure, formed by MO_2 planes separated by R_2O_2 bilayers,[1] gives a strong bidimensional character to the physical properties. The magnetic coupling varies from strong two-dimensional fluctuations to three-dimensional static magnetic ordering.[2] As we show in this paper, the magnetic behavior is very different when an external magnetic field is applied parallel or perpendicular to the *ab* plane. Moreover, due to the mismatch between the two types of layers forming the structure, these compounds undergo different structural phase transitions in order to minimize the resulting strain energy.[3–6]

In the case of R_2NiO_4 compounds (R =La, Pr, or Nd) the structural behavior is characterized by two phase transformations between 1 and 2000 K.[5–9] The transition temperatures vary monotonically with the size of the rare-earth atom. The two observed structural phase transformations are

(i) $I4/mmm \rightarrow Bmab$, $T_{C2} \approx 770$ K for La, 1500 K for Pr, and 1900 K for Nd.

(ii) $Bmab \rightarrow P4_2/ncm$, $T_{C1} \approx 80$ K for La, 117 K for Pr, and 130 K for Nd.

It is worth remarking that in the isomorphous compound La_2CuO_4 only the first (i) phase transition is observed. Nevertheless, a slight doping with Ba, i.e., $La_{2-x}Ba_xCuO_{4+\delta}$ ($x \approx 0.125$) allows the existence of the second (ii) phase transition in a limited range of Ba compositions.[3,4] The superconducting state in this compound is destroyed at the same Ba content.[3]

The dynamics of the low-temperature structural transformation in rare-earth nickelates has been characterized by means of Raman, infrared, and neutron scattering.[10,11,6]

The nickel compounds La_2NiO_4, Pr_2NiO_4 and Nd_2NiO_4 become antiferromagnetically (AF) ordered at $T_{N1} \approx 325 \pm 5$ K, irrespective of the rare-earth atom. The magnetic structure of the Ni sublattice is characterized by a propagation vector $\mathbf{k}=[100]$ and Ni magnetic moments (hereafter spins) oriented along the a axis in a g_x mode.[7–9,12] The isostructural cuprate La_2CuO_4 also orders AF at $T_N \approx 320$ K with the same propagation vector, but in this case the Cu spins point along the b axis ($g_y a_z$ mode).[13] In the case of rare-earth nickelates, the direction of the Ni spin coincides with the tilt axis of the octahedra (i.e.,[100]). In La_2CuO_4 the spin direction and the tilt axis are orthogonal in the basal plane, and that permits the existence of an antisymmetric interaction, which is responsible for the out-of-plane component in the cuprates.[14] Between 80 and 130 K a structural phase transition from low-temperature orthorhombic phase (LTO, space group *Bmab*) to a new low-temperature tetragonal phase (LTT, space group $P4_2/ncm$) takes place in the R_2NiO_4 system. The tilt axis of the NiO_6 octahedra is now along [110] for $z=0$ and $[1\bar{1}0]$ for $z=\frac{1}{2}$.[5–7] The spin arrangement of the LTO phase could, in principle, be modified below T_{C1} to give a ferromagnetic out-of-plane component (f_z). This ferromagnetic component was not observed in neutron powder diffraction

data from La_2NiO_4,[5,8] which established that the canting angle θ of the magnetic moments was smaller than about 5°. Actually, recent data of dc magnetic susceptibility and isothermal magnetization in La_2NiO_4 show the existence of the out-of-plane ferromagnetic component with an angle $\theta \approx 0.14°$.[15] A similar behavior for Nd_2NiO_4 is directly observed by neutron diffraction ($\theta \approx 15°$), below $T_{C1} \approx 130$ K.[9,16] The ordered magnetic moment in the Nd sublattice develops an important ferromagnetic component ($\theta \approx 18°$) below 20 K.

Pr_2NiO_4 shows a different behavior below $T_{C1} \approx 117$ K. Powder neutron-diffraction experiments indicate the existence of an in-plane spin reorientation in a wide temperature range, from 110 to 40 K. At low temperature (1.5 K), the Ni and Pr sublattices are ordered in an antiferromagnetic model $C_x G_y A_z$.[7] Since the magnetic behavior of Pr_2NiO_4 seems to be more complicated than the other nickelates, we decided to study thoroughly its magnetic properties.

The structure of the paper is as follows: The experimental setup is described in the following section. Section III presents the temperature dependence of the magnetic structure for single-crystal neutron diffraction. The isothermal magnetization and dc magnetic susceptibility are examined in Sec. IV. A discussion of the results and the conclusions can be found in Sec. V.

II. EXPERIMENT

A. Crystal growth

The sample was grown by the floating-zone method at the CRPHT-CNRS laboratory in Orléans (France). The procedure has already been described for lanthanum nickelate.[17] In the case of Pr_2NiO_4, the congruent melting at $\approx 1730-1780$ K, which is observed for Pr/Ni=2, allows large bullet-shaped crystals of $Pr_2NiO_{4+\delta}$ to be grown at 1873 K. The growth is made under a flow of Ar, in order to avoid excess oxygen. The samples were stored in an inert atmosphere, in order to avoid possible reaction with atmospheric oxygen and moisture. A reduction process in a mixture of Ar-5%H_2 at 625 K during 48 h produces a stoichiometric sample of 200 mm^3. Samples from the same batch have been used in different experiments presented in this paper. Structure refinements of neutron-diffraction data confirm the complete equivalence in stoichiometry of these single crystals with previous polycrystalline samples ($\delta \approx 0.00 \pm 0.01$).

B. Single-crystal neutron diffraction

Measurements were performed with the four-circle diffractometer D9 at the high-flux reactor of the Institut Laue-Langevin, Grenoble (France). A monochromatic neutron beam with wavelength $\lambda = 0.85$ Å was produced by means of a Cu (220) monochromator in transmission geometry. The higher-order contamination from the monochromator is estimated to be smaller than 1% after the use of an appropriate filter. The sample was attached to the cold finger of a closed-cycle cryostat working from 15 to 300 K with a temperature stability of ±0.5 K. The diffractometer is equipped with a two-dimensional position-sensitive detector with a resolution of 32×32 pixels, which allows an easy measurement of the Bragg reflection accompanied by small satellites and/or twinning peaks (see Ref. 18 for details).

The refinement of the crystal and magnetic structures was carried out with the program MXD.[19] The numbering of Ni and Pr sublattices as well as notation for the description of the magnetic structure is the same as in Refs. 5, 7, and 9.

C. Magnetic measurements

The dc magnetic susceptibility was measured in the temperature range between 1.5 and 300 K for applied fields from 0.4 to 50 kOe. The sample was preoriented using Laue photograph with backscattered x-rays. The magnetic field was applied either along or perpendicular to the c axis with an accuracy better than 1°.

The low-field (smaller than 70 kOe) isothermal magnetization was measured from 1.5 to 300 K in a superconducting quantum interference device (SQUID) magnetometer. The high-field (up to 200 kOe) isothermal magnetization was measured between 4.2 and 30 K by an extraction inductive method at the Service National des Champs Intenses, Grenoble (France).

III. TEMPERATURE DEPENDENCE OF THE MAGNETIC STRUCTURE

The main characteristics of the magnetic structure of Pr_2NiO_4 were described in a previous publication.[7] We shall here concentrate on details that cannot be obtained from powder data. Our single-crystal sample presents a sharp structural phase transition from orthorhombic to tetragonal at $T_{C1} = 117$ K. At low temperature (15 K) the structure belongs to the $P4_2/ncm$ space group with lattice parameters $a = 5.49(1)$ Å and $c = 12.17(2)$ Å.[20]

It is worth mentioning that some authors have claimed the existence of a phase in the $Pr_2NiO_{4+\delta}$ system (with $\delta \approx 0.06$) having the $P4_2/ncm$ symmetry in the whole temperature range below room temperature (RT).[21] We have not been able to obtain such a kind of sample in any of our trials. As the authors show, the sample used in Ref. 21 is not single phase and we are tempted to think that the reflection violating the *Bmab* (or *Fmmm*) extinction rules corresponds to an average phase (not well characterized yet), which has nothing to do with the LTT ($P4_2/ncm$) phase.

Our single crystal, except for minor details, presents the same overall structural and magnetic behavior as our previous polycrystalline samples.[7] The temperature dependence of the integrated intensity of the main magnetic Bragg reflections are presented in Figs. 1 and 2.

As previously described,[7] the three-dimensional AF ordering of the Ni sublattice occurs at $T_{N1} = 325$ K. This value is close to that obtained for the isomorphous compounds La_2NiO_4 and Nd_2NiO_4.[5,8,9] We suspect that the value of T_{N1} quoted in the literature[22] for La_2NiO_4 ($T_{N1} \approx 650$ K) is wrong. As this temperature (650 K) is close to the Curie temperature of bulk metallic Ni and of small Ni particles,[23] the anomaly in the susceptibility will

be most certainly related to the presence of small metallic Ni precipitates arising from an excess of reduction.

The magnetic structure between T_{N1} and T_{c1} corresponds to a pure g_x mode with the moments aligned along the a axis, giving its strongest contribution to the (011) magnetic reflection. Since the orthorhombic structure is derived from a high-temperature tetragonal $I4/mmm$ phase, two crystallographic twins exist. The small intensity observed for the position of the (101) reflection in Fig. 2, forbidden in a g_x mode, originates from the second twin of the (011) magnetic reflection. Similar arguments apply for the pair of reflections (013) and (103). The data presented in Figs. 1 and 2 were obtained in different thermal cycles. As no thermal hysteresis was observed, no distinction has been made in the plots between different heating and cooling processes. Instead, we show an average between those measurements. At low temperature (15 K), the magnetic mode of the Ni sublattice is $c_x g_y a_z$, and the Pr sublattice is ordered in the same mode. Table I summarizes the low-temperature refined magnetic moments and the crystallographic data.

The change from g_x to $c_x g_y a_z$ corresponds to a magnetic phase transition taking place at $T_{N2}=90$ K. There was only a weak indication of this transformation in previous powder data. However, ac susceptibility measurements in a small Pr_2NiO_4 single crystal from the same bullet clearly show an anomaly associated with this phase transformation.[24]

In the temperature range between $T_{c1}=117$ K and $T_{N2}=90$ K there is a spin reorientation process. Due to the structural phase transformation at T_{c1}, the magnetic modes g_x and $c_y f_z$ are mixed, as discussed in Ref. 7. Due to the average tetragonal crystal structure, it is difficult to determine the magnetic symmetry of the Ni sublattice. Two possibilities exist, tetragonal $P4_2/nc'm'$ ($g_x + c_y f_z$), which implies that the in-plane component of the spin is along the [110] direction for $z=0$ and along the $[1\bar{1}0]$ direction for $z=\frac{1}{2}$. The other possibility is the multidomain orthorhombic $Pc'c'n$ ($g_x c_y f_z$) with magnetic moments mainly along the x direction. It is difficult to separate the two cases, even using single-crystal diffraction. Only the application of an external magnetic field could help to distinguish between both cases. The in-plane spin reorientation below T_{c1} from g_x to $g_x c_y$ (or $g_x + c_y$) is clearly observed from the temperature dependence of the (013), (103), (011), and (101) magnetic reflections (Figs. 1 and 2). Between $90 < T < 117$ K the

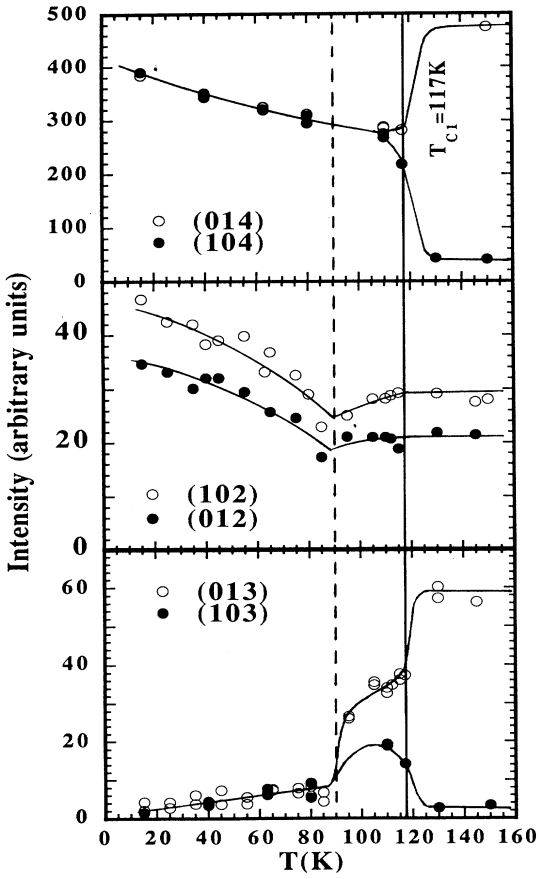

FIG. 1. Temperature dependence of the (014), (104), (012), (102), (013), and (103) magnetic reflections for Pr_2NiO_4 showing the structural phase transition at $T_{c1}=117$ K (vertical solid line) and the magnetic phase transformation at $T_{N2}=90$ K (vertical dashed line). the lines are guides to the eye.

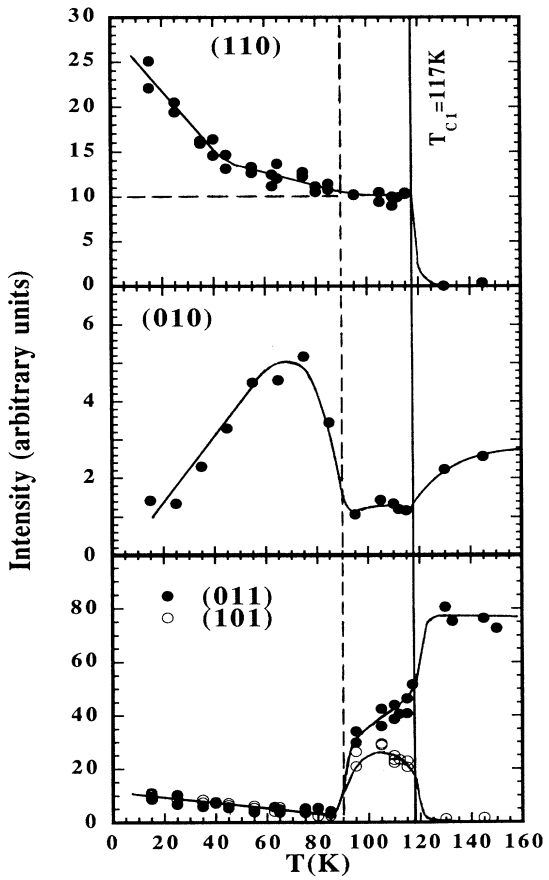

FIG. 2. As in Fig. 1 for the (110), (010), (100), (011), and (101) magnetic reflections.

TABLE I. Refined crystallographic parameters for Pr_2NiO_4 single-crystal neutron diffraction at 15 K, $b_O = 5.805$ fm, $b_{Ni} = 10.3$ fm, and $b_{Pr} = 4.45$ fm. The magnetic moments have been measured at 1.5 K. Magnetic form factor for Ni has been refined from Ref. 28 and for Pr from Ref. 29. $a = 5.49(1)$ Å, $c = 12.17(2)$ Å. Numbers in parentheses indicate standard deviations in the last digit. $R = 0.036$, $R_W = 0.054$.

Atom	x	y	z	Total magnetic moment (μ_B)	In plane (μ_B)	Out of plane (μ_B)	Canting angle (deg)
Pr	−0.0129(2)	−0.0129(2)	0.3634(1)	1.09(5)	0.9(1)	0.66(6)	80(4)
Ni	0	0	0	1.44(7)	1.4(1)	0.3(1)	127(3)
O(1)	$\frac{1}{4}$	$\frac{1}{4}$	−0.0281(1)				
O(1)′	$\frac{3}{4}$	$\frac{1}{4}$	0				
O(2)	0.0497(2)	0.0497(2)	0.17835(9)				

intensity of (013) and (011) decreases accompanied by a corresponding increase of the (103) and (101) magnetic reflections.

At $T_{N2} = 90$ K a magnetic phase transition takes place from the $g_x c_y f_z$ magnetic structure to $c_x g_y a_z$. The phase transition is specially apparent from the sudden decrease in intensity observed for the pairs of reflections (013)-(103) and (011)-(101) reflections. Moreover, there is a sudden upward jump in the intensity of the (010) and (100), and a smooth increase of the (012) and (102) reflections. The low-temperature magnetic structure has an AF out-of-plane component (a_z), similar to that observed in La_2CuO_4. This is seen from the intensity of the (110) Bragg reflection. For $T > T_{c1}$ this reflection is forbidden, while it has nuclear and magnetic contributions below T_{c1}. The nuclear contribution is represented by the horizontal dashed line in Fig. 2. It is only below 90 K that the (110) intensity increases.

At low temperature the Pr sublattice becomes ordered within the same irreducible representation as the Ni sublattice. This means that the coupling between both kinds of sublattices is responsible of the global magnetic-moment configuration. The ordering temperature of the Pr sublattice is very difficult to determine. In principle, the (014) and (104) magnetic reflections are mainly sensitive to the Pr ordering due to their relatively high Bragg angle (the Ni form factor falls off faster with the scattering angle). Figure 1 suggests that there is an ordered magnetic moment in Pr sites below $T_{c1} = 117$ K. However, its amplitude is very small and difficult to estimate. The ordered moment becomes significant below 40 K, where a change in the slope of the (110) reflection is observed, associated with the growing of the AF out-of-plane component on the Pr sublattice. The low-temperature intensity of both (014) and (110) reflections is not saturated. Moreover, the magnetic moment of Pr at 15 K is much smaller than that expected for a free ion (3.58 μ_B). All these observations indicate that the ordered magnetic moment of Pr ions is induced by the local exchange field coming from the Ni sublattice.

IV. MAGNETIC PROPERTIES

Figure 3 shows the magnetic susceptibility of the Pr_2NiO_4 crystal, measured in magnetic fields applied parallel to the c axis of values 430 Oe [Fig. 3(b)] and between 25 and 50 kOe [Fig. 3(a)]. The following points have to be emphasized upon inspection of both figures. For temperatures higher than T_{c1}, the magnetic susceptibility is dominated by the paramagnetic moment of Pr. The Ni sublattice is AF ordered below RT and its contribution to the susceptibility is very small. The effective paramagnetic moment of Pr^{3+} calculated from RT to T_{c1} is 3.1 μ_B lower than the expected value (3.58 μ_B), and slightly dependent on the applied magnetic field.

The structural phase transition is observed as a discon-

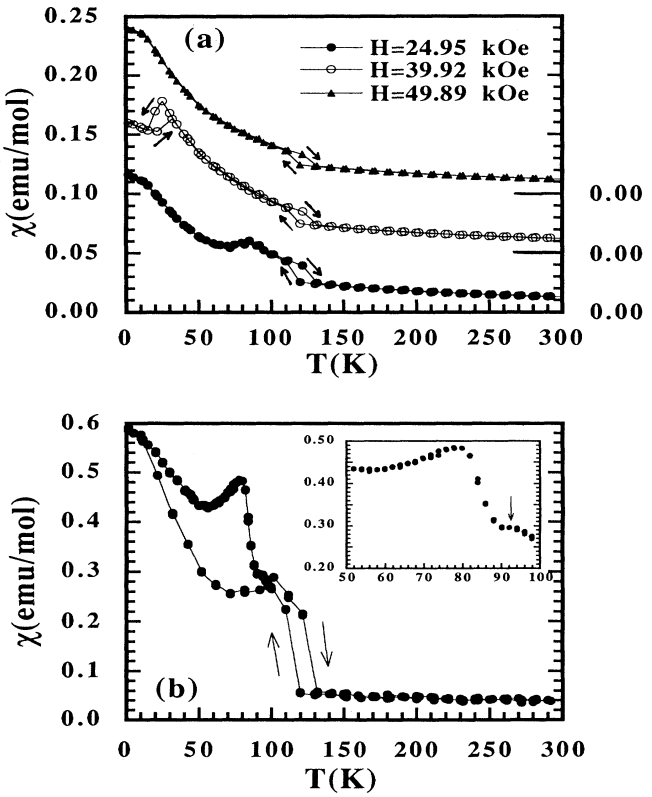

FIG. 3. Temperature dependence of the magnetic dc susceptibility for different external magnetic fields applied parallel to the crystallographic c axis for cooling and heating process. (a) $25 < H < 50$ kOe, (b) $H = 430$ Oe. The inset shows the details between 50 and 100 K.

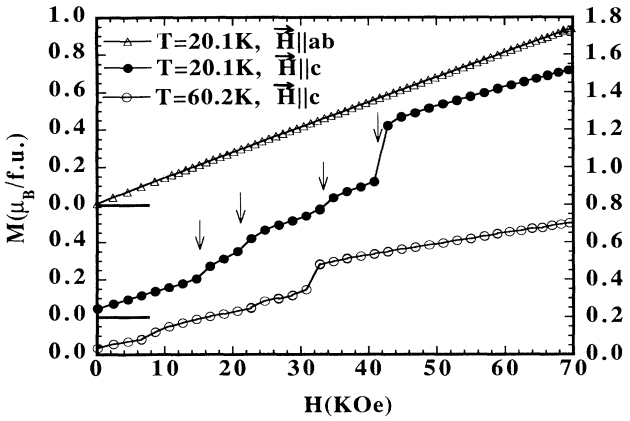

FIG. 4. Magnetization isotherms vs magnetic field at different temperatures for the magnetic field applied parallel to the *ab* plane and applied parallel to the *c* axis.

tinuous jump due to the appearance of the ferromagnetic component at T_{c1}. This transition presents a thermal hysteresis (≈ 10 K wide) as a signature of its first-order character.

Below T_{c1} and for fields above 5 kOe a peak in the magnetic susceptibility is seen [Fig. 3(a)]. This peak also presents thermal hysteresis (≈ 10 K) and is certainly related to the metamagnetic transitions described below.

The broad maximum at 80 K in the data for $H = 430$ Oe [Fig. 3(b)] has a different origin and it was observed in previous dc magnetization data at very low fields (5 Oe) on polycrystalline samples.[7] The thermal cycling around the transition temperature T_{c1} induces a variation of 20 K in the position of the maximum and its amplitude changes by a factor of 2. The origin of this feature has not been yet elucidated. There is an additional small peak at 92 K [see inset Fig. 3(b)], which can be related with similar features observed at stronger applied magnetic fields. On thermal cycling this small peak also shows a hysteresis of about 10 K.

The isothermal magnetization is presented in Fig. 4 for low magnetic fields. The first important point is its

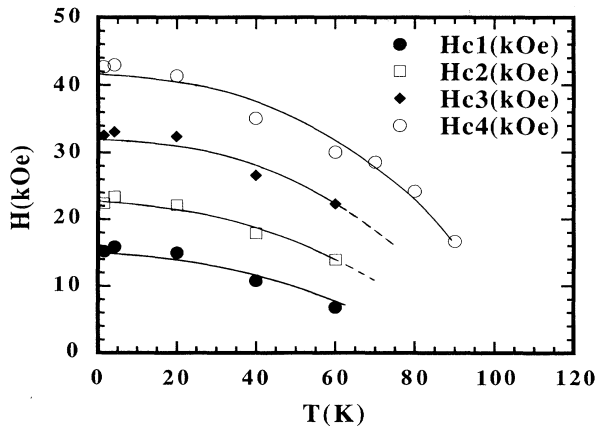

FIG. 5. Temperature dependence of the different field-induced transitions in Pr_2NiO_4 below $T_{N2} = 90$ K.

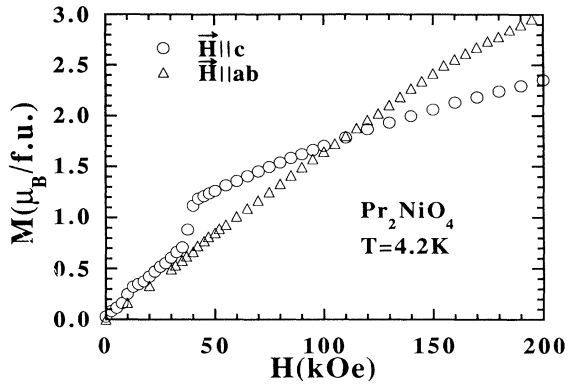

FIG. 6. Isothermal magnetization for a high magnetic field applied parallel and perpendicular to the crystallographic *c* axis.

linear field dependence obtained when the magnetic field is applied perpendicular to the *c* axis (within the *ab* plane), in the full temperature range from 1.5 to 300 K. When the applied field is parallel to the *c* axis, and $T > T_{c1}$, a linear field dependence is also observed (not shown). On the contrary, for $T < T_{c1}$, there is evidence of several field-induced transitions. On increasing the applied magnetic field, a series of three small jumps precedes a larger jump at higher fields (Fig. 4). The temperature dependence of the critical fields producing the jumps in magnetization is presented in Fig. 5. The field-induced transitions are clearly observed up to 60 K, while from 60 K to T_{c1} only a smooth curvature is manifested.

The high-field isothermal magnetization at 4.2 K is shown in Fig. 6. In the case of the applied field being perpendicular to the *c* axis only a change in the slope appears at $H \approx 150$ kOe, probably associated with a spin-flop transition similar to that observed in La_2CuO_4.[25] Since the relative orientation between the spin direction and the external field is not exactly known, no more details can be obtained from the present data. When the applied field is parallel to the *c* axis, two transitions are observed at 16 and 42 kOe. The intermediate field-induced transitions (at 23 and 33 kOe) observed in the low-field data (Fig. 4) were probably not seen because the crystal was aligned with an estimated precision of $\pm 10°$. Nevertheless, the magnetization jumps at both critical fields (16 and 42 kOe) correspond to those observed at lower fields. The higher zero-field extrapolated moment is observed for magnetic fields higher than 130 kOe, with a value of 1.2 μ_B per formula unit.

The zero-field extrapolated moment corresponding to the jumps in magnetization as well as the corresponding magnetic fields at 1.5 K for each transition are $M_1 = 0.12 \pm 0.05 \mu_B$/f.u., $H_{c1} = 16 \pm 1$ kOe; $M_2 = 0.3 \pm 0.1 \mu_B$/f.u., $H_{c2} = 23 \pm 1$ kOe; $M_3 = 0.4 \pm 0.1 \mu_B$/f.u., $H_{c3} = 33 \pm 1$ kOe; and $M_4 = 0.95 \pm 0.05 \mu_B$/f.u., $H_{c4} = 42.3 \pm 0.5$ kOe. The M_4 value increases until $1.20 \pm 0.02 \mu_B$/f.u. if we take into account the high-field data.

V. DISCUSSION AND CONCLUSIONS

The three-dimensional (3D) ordering of the Ni sublattice in Pr_2NiO_4 takes place at a Néel temperature of 325

K. Between that temperature and 117 K, where the LTO-LTT phase transition occurs, the spin arrangement corresponds to a g_x mode. The same AF ordering has been found in the two other studied nickelates, La_2NiO_4,[5] and Nd_2NiO_4.[9] The isostructural cuprate La_2CuO_4 presents, by contrast, a $g_y a_z$ arrangement.[13]

The subtle interplay between the different magnetic interactions giving rise either to the La_2CuO_4 and La_2NiO_4 magnetic structures has not been determined yet (see, for instance, Ref. 26). Up to first order, the single-ion anisotropy of Cu^{2+} ($S=\frac{1}{2}$) does not contribute to the spin Hamiltonian (see Ref. 14). Probably the magnetocrystalline (single-ion) anisotropy of Ni^{2+} ($S=1$), as well as dipolar or pseudodipolar interactions, plays a role in stabilizing the g_x mode with respect to the mode $g_y a_z$. This point deserves a deeper investigation.

The Néel temperature is nearly independent of the rare-earth cation or the transition metal: the four critical temperatures for the referred isomorphous compounds all lie between 320 and 330 K. On the other hand, it depends strongly on the oxygen stoichiometry, probably as a result of competition between ferro- and antiferromagnetic interactions generated either by the presence of low-spin Ni^{III} with empty $d_{x^2-y^2}$ orbitals, or localized holes in oxygen sites. Single-crystal $Pr_2NiO_{4+\delta}$ neutron-diffraction data, for intermediate oxygen concentration ($\delta=0.06$), show a decrease in the ordering temperature down to 116 K, and a strong reduction of the ordered moment for Ni^{2+} ($0.62\mu_B$ at 10 K) and Pr^{3+} ($0.30\mu_B$ at 10 K).[21]

The saturation magnetization as obtained from the extrapolation of the high fields to $H=0$ from data of Fig. 4 depends on temperature as indicated in Fig. 7. From T_{c1} to 40 K a linear behavior is observed. Below 40 K a pronounced increase in the magnetization is evident, probably related with the appearance of a significant ordered moment associated with the Pr sublattice.

The behavior below T_{c1} of Pr_2NiO_4 is closer to that of Nd_2CuO_4 than that of Nd_2NiO_4. Magnetic susceptibility and magnetization measurements show the appearance of a weak ferromagnetic component along the z direction,

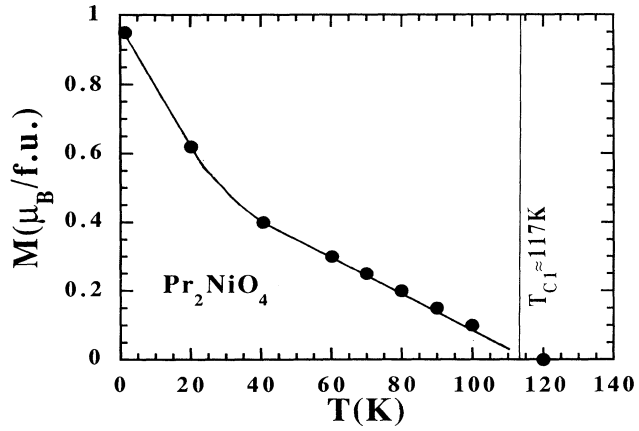

FIG. 7. Zero-field extrapolated moment vs temperature for Pr_2NiO_4 as derived from isothermal magnetization data.

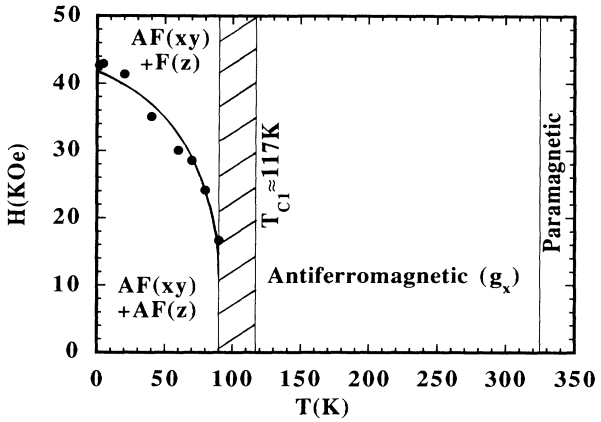

FIG. 8. Magnetic-field temperature phase diagram for Pr_2NiO_4 showing the different regions: Paramagnetic ($T > T_{N1}=325$ K), antiferromagnetic with magnetic moments along the x direction ($T_{c1}=117$ K $< T < T_{N1}=325$ K), in-plane spin reorientation ($T_{N2}=90$ K $< T < T_{c1}=117$ K, and for $T < T_{N2}=90$ K, the metamagnetic transformation in which the out-of-plane component changes from an antiferromagnetic ordering to a ferromagnetic ordering, while the xy plane remains antiferromagnetically ordered.

which is too small to be observed by neutron diffraction. From this moment, the temperature dependence of the magnetic structure of Pr_2NiO_4 is qualitatively different from that of the isomorphous compounds La_2NiO_4 and Nd_2NiO_4. At about 90 K, Pr_2NiO_4 shows a spin reorientation bearing the appearance of an a_z component, that gives a spin ordering similar to the La_2CuO_4 magnetic structure. Considering this out-of-plane component, the resultant arrangement can be described as planes in which the z component of magnetic moments are ferromagnetically ordered, with an antiferromagnetic disposition between the planes. As stated above, magnetic phase transitions in the transition-metal sublattice presenting the same phenomenology have been observed in Nd_2CuO_4.[2,27] In this case, the Cu^{2+} ions are surrounded by square planes of oxygen and no structural transition is observed below RT. There is a magnetic phase transition at $T_{N2}=75$ K, where the spin arrangement changes from the La_2NiO_4 type to the La_2CuO_4 type. At a lower temperature, $T_{N3}=30$ K, the magnetic structure reverts to the La_2NiO_4 type. Around this temperature a small ordered magnetic moment in Nd sublattice starts to develop. At 0.4 K, the magnetic moment of the Nd^{3+} ion is $1.3\mu_B$, far from the free-ion value ($3.27\mu_B$).[2]

When an external magnetic field is applied parallel or perpendicular to the c axis in Pr_2NiO_4 for $T > T_{c1}$, the obtained dependence of the magnetization is typical of a collinear antiferromagnetic system.

For temperatures below T_{c1} and the magnetic field applied perpendicular to the z direction (within the ab plane), a conventional linear dependence on H is observed. On the other hand, when the direction of the external field is along [001], a jump appearing in the magnetization indicates the existence of a metamagnetic tran-

sition. At this transition the planes order ferromagnetically, with respect to the out-of-plane component. The magnetic structure is then antiferromagnetically ordered in the xy planes and ferromagnetically in the z direction. At low temperatures it can be seen that this jump is preceded by other anomalies, suggesting that the metamagnetic transition takes place in several stages with intermediate magnetic structures. It is not possible to determine those intermediate spin arrangements from these magnetization measurements. A neutron-diffraction experiment under applied external magnetic field will be performed shortly to obtain the different steps in the metamagnetic transition as well as the precise final magnetic structure. A preliminary phase diagram H vs T, which condenses our present knowledge of the magnetic properties of this system is presented in Fig. 8.

The set of magnetic interactions, as well as their temperature dependence, governing the magnetic phase transitions taking place in Pr_2NiO_4 and Nd_2CuO_4 needs to be studied thoroughly in order to determine the reason(s) for similarities found between these two compounds. Such a study should also shed light on the overall magnetic behavior of the whole system of nickelates and cuprates belonging to the two structural types. An investigation on the theoretical models in this sense is under way.

ACKNOWLEDGMENT

The Institut Laue-Langevin is acknowledged for making available the neutron beam time.

---

*Present address: Instituto de Ciencia de Materiales de Madrid (sede B), C.S.I.C. Fac. Ciencias (C-4), Universidad Autónoma de Madrid, E-28049 Madrid, Spain.

†Present address: Laboratoire Léon Brillouin (CEA), CE-Saclay, F-91151 Gif-sur-Yvette, France.

[1]H. Müller-Buschbaum, Angew. Chem. Int. Ed. Engl. **30**, 723 (1991).

[2]M. Matsuda, K. Yamada, K. Kakurai, H. Kadowaki, T. R. Thurston, Y. Endoh, Y. Hidaka, R. J. Birgeneau, M. A. Kastner, P. M. Gehring, A. H. Moudden, and G. Shirane, Phys. Rev. B **42**, 10098 (1990).

[3]J. D. Axe, A. H. Moudden, D. Hohlwein, D. E. Cox, K. M. Mohanty, A. R. Moodenbaugh, and Xu Youwen, Phys. Rev. Lett. **62**, 2751 (1989).

[4]P. Böni, J. D. Axe, G. Shirane, R. J. Birgeneau, D. R. Gabe, H. P. Jenssen, M. A. Kastner, C. J. Peters, P. J. Picone, and T. R. Thurston, Phys. Rev. B **38**, 185 (1988); R. J. Birgeneau *et al.*, Phys. Rev. Lett. **59**, 1329 (1987); T. R. Thurston *et al.*, Phys. Rev. B **39**, 4327 (1989).

[5]J. Rodríguez-Carvajal, M. T. Fernández-Díaz, and J. L. Martínez, J. Phys. Condens. Matter **3**, 3215 (1991).

[6]J. L. Martínez, M. T. Fernández-Díaz, J. Rodríguez-Carvajal, and P. Odier, Phys. Rev. B **43**, 13766 (1991).

[7]M. T. Fernández-Díaz, J. Rodríguez-Carvajal, J. L. Martínez, G. Fillion, F. Fernández, and R. Saez-Puche, Z. Phys. B **82**, 275 (1991).

[8]R. Saez-Puche, F. Fernández, J. L. Martínez, and J. Rodríguez-Carvajal, J. Less Common Met. **149**, 357 (1989).

[9]J. Rodríguez-Carvajal, M. T. Fernández-Díaz, J. L. Martínez, F. Fernández, and R. Saez-Puche, Europhys. Lett. **11**, 261 (1990).

[10]A. de Andrés, J. L. Martínez, and P. Odier, Phys. Rev. B **45**, 12821 (1992).

[11]D. E. Rice, M. K. Crawford, D. J. Buttrey, and W. E. Farneth, Phys. Rev. B **42**, 8787 (1990); see also, G. Burns, F. H. Dacol, D. E. Rice, D. J. Buttrey, and M. K. Crawford, *ibid.* **42**, 10777 (1990).

[12]G. Aeppli and D. J. Buttrey, Phys. Rev. Lett. **61**, 203 (1988); G. H. Lander, P. J. Brown, C. Stassis, P. Gopalan, J. Spalek, and G. Honig, Phys. Rev. B **43**, 448 (1991).

[13]M. A. Kastner, R. J. Birgeneau, T. R. Thurston, P. J. Picone, H. P. Jenseen, D. R. Gabbe, M. Sato, K. Fukuda, S. Shamoto, Y. Endoh, K. Yamada, and G. Shirane, Phys. Rev. B **38**, 6636 (1988).

[14]D. Coffey, J. Appl. Phys. **70**, 6326 (1991).

[15]X. Batlle, X. Obradors, M. J. Sayagués, M. Vallet, and J. Gonzalez-Calbet, J. Phys. Condens. Matter **4**, 487 (1992).

[16]X. Obradors, X. Batlle, J. Rodríguez-Carvajal, J. L. Martínez, M. Vallet, J. González-Calbet, and J. Alonso, Phys. Rev. B **43**, 10451 (1991).

[17]K. Dembinski, J. M. Bassat, J. P. Coutures and P. Odier, J. Mater. Sci. Lett. **6**, 1365 (1987).

[18]M. S. Lehmann, W. E. Kuhs, G. J. MacIntyre, C. Wilkinson, and J. R. Allibon, J. Appl. Crystallogr. **22**, 562 (1989).

[19]P. Wolfers, J. Appl. Crystallogr. **23**, 553 (1990).

[20]M. T. Fernández-Díaz, J. Rodríguez-Carvajal, J. L. Martínez, and P. Odier, Physica B **180-181**, 122 (1992).

[21]D. J. Buttrey, J. D. Sullivan, G. Shirane, and K. Yamada, Phys. Rev. B **42**, 3944 (1990).

[22]P. Gopalan, M. W. McElfresh, Z. Kakol, J. Spalek, and J. M. Honig, Phys. Rev. B **45**, 249 (1992).

[23]Y. Du, M. Xu, J. Wu, Y. Shi, H. Lu, and R. Xue, J. Appl. Phys. **70**, 5903 (1991).

[24]X. Obradors, B. Martínez, X. Batlle, J. Rodríguez-Carvajal, M. T. Fernández-Díaz, J. L. Martínez, and P. Odier, J. Appl. Phys. **70**, 6329 (1991).

[25]T. Thio, T. R. Thurston, N. W. Preyer, P. J. Picone, M. A. Kastner, H. P. Jenseen, D. R. Gabbe, C. Y. Chen, R. J. Birgeneau, and A. Aharony, Phys. Rev. B **38**, 905 (1988); T. Thio, C. Y. Chen, B. S. Freer, D. R. Gabbe, H. P. Jenssen, M. A. Kastner, P. J. Picone, N. W. Preyer, and R. J. Birgeneau, *ibid.* **41**, 231 (1990).

[26]K. Yamada, T. Omata, K. Nakajima, S. Osoya, T. Sumida, and Y. Endoh, Physica C **191**, 15 (1992).

[27]S. Skanthakumar, H. Zhang, T. W. Clinton, I. W. Sumarlin, W-H. Li, J. W. Lynn, Z. Fisk, and S-W. Cheong, J. Appl. Phys. **67**, 4530 (1990), and references therein.

[28]P. J. Brown (unpublished).

[29]M. Blume, A. J. Freeman, and R. E. Watson, J. Chem. Phys. **37**, 1245 (1962). We have calculated the form factor for Pr within the dipole approximation.